Materials Research Proceedings 38 (2023) 141-149 https://doi.org/10.21741/9781644902837-20

Computational Modeling of PM-HIP Capsule Filling and Consolidation by DEM-FEA Coupling

S. Sobhani[1,2,a*], M. Albert[3,b], D. Gandy[3,c], A. Tabei[1,2,d], A. Fan[1,2,e]

[1]School of Mechanical, Industrial, and Manufacturing Engineering, Oregon State University, Corvallis OR, USA

[2]Advanced Technology and Manufactruing Institute (ATAMI), Oregon State University, Corvallis OR, USA

[3]Electric Power Research Institute (EPRI), Charlotte NC, USA

[a]sobhanis@oregonstate.edu, [b]malbert@epri.com, [c]davgandy@epri.com, [d]ali.tabei@gmail.com, [e]zhaoyan.fan@oregonstate.edu

Keywords: Hot Isostatic Pressing (HIP), Modeling, Discrete Element Method, Finite Element Analysis, Capsule Filling

Abstract. Power Metallurgy Hot Isostatic Pressing (PM-HIP) is a manufacturing process, capable of producing net shape or near net shape components with complicated geometries from materials that are often difficult to cast and/or deform. However, the post-HIP quality and requirement of any additional process, such as machining, depends on the design and geometric complexity of the capsule. First of a kind geometry often requires several iterations of prototype builds. Considering the cost and long durations of HIP cycles, usage of computer models in order to predict parameters for an optimal capsule design of a PM-HIP process which produces a sound product in *the first trial* is extremely valuable. In this study, the pre-consolidation capsule filling process is simulated by Discrete Element Method (DEM) to capture the initial relative density. Finite element analysis (FEA) modeling of HIP, which includes a combined constitutive model based on compressive and consolidative mechanical behavior of powder uses the DEM results as input. Accuracy of the simulation tool is confirmed by comparing against a corresponding physical PM capsule fabrication and HIP experiment with pre- and post-HIP 3D scanning. The result shows that consolidation occurs as the model predicts, with negligible deviations on sharp edges.

Introduction

In HIP, a thin-walled capsule is filled with metal/alloy powder. After that the capsule is sealed and outgassed and then goes under a high-pressure and high-temperature HIP cycle for a given duration, usually in the order of 2 to 4 hours. The high pressures and temperatures lead to a noticeable shrinkage and deformation of the capsule [4,5] resulting in a near net-shaped part/component. A slight deviation in HIP parameters and factors can result in both microstructural and/or geometrical anomalies in the final produced part/component [6].

The filling step and early stages of the HIP process often involve the use of atomized metal powders; therefore, the Discrete Element Method (DEM) is the appropriate tool for modeling purposes [7]. At later stages of HIP where some degree of consolidation happens, FEA is more prominent in predicting the behavior and more applicable for to continuum models [7–13].

One of the more critical input parameters in the HIP process is the relative density (RD), the ratio of the density of the powder compact to the density of the bulk material. Accordingly, the central phenomenon of the HIP process is the evolution of RD to unity. Therefore, understanding RD distributions of the pre- and post-HIP parts are critical for a robust prediction of the shape of the final compact (solidified powder) and behavior of metal powders during the process [2, 3].

Materials Research Proceedings 38 (2023) 141-149 https://doi.org/10.21741/9781644902837-20

According to the literature, the RD in filled HIP capsules may vary between 54% to 74% depending on the metal powder properties, filling procedure parameters, and the geometry of the capsule [14]. Previous studies have shown that establishment of a homogenous RD for the powder can help to achieve more accurate design of the component [8, 15]. The evolution of RD is a direct function of the volume change (consolidation/shrinkage), which is related to permanent deformation of the compact [16, 17]. Abouaf [5] developed an incremental and implicit finite element algorithm for compressing metal powders. It was proposed to extend the previous porous material plasticity theories of Oyane et. al. [18] and Kuhn [19] to capture complexities of HIP. The additional deformation in HIP was captured by accounting for creep, as the component is exposed to high temperatures.

Wickman et. al. [20] looked to develop a numerical simulation method to predict the final shape of the HIP'ed products by focusing on reducing the cost of the final parts by reducing the amount of machining required. Rate-dependent (viscoplastic) and rate-independent deformations were considered in this study. Based on dilatometry experiments, considerable deformation and particle rearrangement occurred during the early stages of HIP. However, due to fitting the viscoplastic deformation parameters to the entire process, the final axial deformation showed larger deformation. Van Nguyen and coworkers [8], discussed the importance of the density distribution, local RD gradient and knowledge of the amount of RD in improving the deformation and shrinkage during the HIP stages.

To investigate the effects of filling parameters on RD, three different capsule filling methods: 1) benign filling, 2) filling with tapping and 3) filling with vibration; were considered. The result suggested that near net shape parts require a stable powder particle size distribution, good mixing, and homogenous density gradient (close range of RD). Each of these are obtainable by conducting filling with tapping and vibrations.

In the current study, the pre-consolidation capsule filling process is simulated by discrete element method (DEM) to capture the initial relative density. Then FEA modeling of the HIP process with the DEM results as an input was used. This modeling includes a combined constitutive model based on mechanical behavior of the powder during compaction and consolidation in conjunction.

Methodology

1. Discrete Element Method (DEM)

DEM is a numerical technique based on a set of motion equations to model the movement and flow behavior of granular media [21,22]. DEM is founded on analyze forces due to particle-particle and particle-wall interaction [23,24]. The motion of each particle is captured by the Newton's second law. Therefore, for particle i in a body of powder, the following equations are derived:

$$m_i \frac{dv_i}{dt} = m_i g + \sum_{i=1}^{n} \left(F_{n,ij} + F_{t,ij}\right) \tag{1}$$

$$I_i \frac{d\omega_i}{dt} = \sum_{i=1}^{n} (T_{t,ij} + T_{r,ij}) \tag{2}$$

Where m_i is the mass of particle i and n represents the total number of particles in the system. v is velocity. F_t and F_n are respectively the tangential and normal contact force components. I_i is the moment of inertia of particle i, ω is angular velocity, and T_t, T_r are respectively the tangential and rolling torque [25]. In HIP process, particles have compressible plastic behavior, therefore Hysteretic Linear Spring Contact model is chosen to use in this work, due to its capability to show

Materials Research Proceedings 38 (2023) 141-149 https://doi.org/10.21741/9781644902837-20

acceptable model for the granular material. Hysteretic Linear Spring Contact Model (HLSC) is based on the formalism proposed by Walton and Braun [26].

2. Constitutive model

For the FEA simulation used in this research, a combined constitutive model that can capture the complexities of the various active mechanisms in an acceptable way, is presented by Van Nguyen et. al. [29]. This combined model is based on the rate-dependent model by Abouaf [32] and Kuhn's and Downey's time-independent plasticity model [33]. In this model plastic yielding, linear isotropic hardening, and viscoplastic deformation lead to volume shrinkage and densification. The total strain developed in the powder is decomposed as follows:

$$\varepsilon_{ij} = \varepsilon_{ij}^{el} + \varepsilon_{ij}^{inel} + \varepsilon_{ij}^{th} \tag{3}$$

$$\varepsilon_{ij}^{inel} = \varepsilon_{ij}^{pl} + \varepsilon_{ij}^{cr} \tag{4}$$

Where ε_{ij} is total strain and $\varepsilon_{ij}^{el}, \varepsilon_{ij}^{inel}, \varepsilon_{ij}^{th}$ are elastic strain, inelastic strain and thermal strain. The inelastic strain is then decomposed into ε_{ij}^{pl} and ε_{ij}^{cr} which represent plastic and creep strains. Both primary and secondary creep mechanisms are considered in the creep strain term. Based on Kuhn's and Downey's work [19], an ellipsoidal yield surface which is a modified form of Von Mises criterion was used in the combined model. The yield function f is described by the following equations:

$$_{i}, \rho, \varepsilon_p) = \sigma_{eq}\text{-}r_1(\rho, p) - \sigma_y(\rho) = [A(\rho)\, J_2 + B(\rho) I_1^2]^{1/2} - h\rho^m - \sigma_0 \rho^k \tag{5}$$

Where σ_{eq} is the equivalent plastic stress that is a function of Cauchy stress components and the relative density via the $A(\rho)$ and $B(\rho)$, which are themselves functions of the relative density and the plastic Poisson ratio v_{pl}. In linear isotropic hardening, $r_1(\rho, p)$, which the relative density (ρ) and equivalent plastic strain (ε_p) [30] had an impact linear hardening for porous materials.

The tangential modulus h and exponent m are obtained by uniaxial compression experiments. $\sigma_y(\rho)$ is the initial yield stress which is a function of relative density, ρ. σ_0 is the yield stress in the fully dense material and k is a parameter obtained from detailed experiments.

Time independent inelastic deformation via creep, based on the Abouaf et. al. [32] creep model is used in this study. The creep rate ($\dot{\varepsilon}_{ij}^{cr}$) for porous materials is represented in the form of:

$$\dot{\varepsilon}_{ij}^{cr} = A(T)\sigma_{eq2}^{N(T)-1}\left(\frac{3}{2}c(\rho)S_{ij} + f(\rho)I_1\delta_{ij}\right) \tag{6}$$

Where A(T) is a function of temperature, $N(T)$ is the Dorn's constant parameter and $c(\rho)$ and $f(\rho)$ are experimental values measured as functions of relative density. σ_{eq} represented the equivalent stress due to creep deformation [34].

$$\sigma_{eq}^2 = 3c(\rho)J_2 + f(\rho)I_1^2 \tag{7}$$

Materials Research Proceedings 38 (2023) 141-149 https://doi.org/10.21741/9781644902837-20

Thermal strain increment is calculated as follows:

$$\Delta\varepsilon_{ij}^{th} = \alpha_{th}.\Delta T.\delta_{ij} \quad (8)$$

Where $\alpha_{th}$is the thermal expansion coefficient that depends on relative density and temperature. $\Delta T$and δ_{ij} are respectively, the change in temperature and the Kronecker's delta[29][15,34].

The density and temperature dependent model described above was coded in FORTRAN. As mentioned before, initial relative density values were transferred from DEM simulations; then input into the finite element analysis software ANSYS, through the User Programmable Feature (UPF) capability of ANSYS. ANSYS calculation engine solves for location dependent stresses and strains [35] for every timestep via Newton-Raphson iteration and updates density, ρ , accordingly based on the Eq. 8.

$$\rho^{t+\Delta t} = \rho^{t} \exp\left(\Delta\varepsilon_{kk}^{ine}\right) \quad (9)$$

3. Application of the Model

In the current study, the combined DEM and FEA models are used to simulate the HIP compaction of an example capsule geometry which can then be compared to experimental physical HIP capsule and 316L components. The application starts with investigating the initial density from the pre-consolidation process using DEM software. The 3D geometry used for the DEM part is shown in Fig. 1. (for the FEA simulation, a 2D axisymmetric figure is used to reduce the computational times since the component is symmetric around the Z axis). The particle distribution curve of the 316L powder is shown in Fig. 2. The pre-consolidation powder filling parameters such as time, and vibrational setups (frequency and amplitude) has been considered as 15 minutes, 60 HZ and 5 mm. The DEM filling simulation then provides an initial density that is transferred to the FEA model for stainless steel 316L. The material constants for the aforementioned equations are simulated with FORTAN code and the final dimensions of the capsule can be evaluated with experiment results.

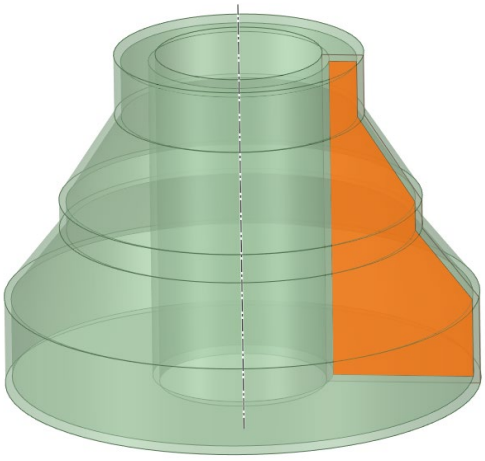

Figure 1. 3D model and 2D axisymmetric geometry

Materials Research Proceedings 38 (2023) 141-149 https://doi.org/10.21741/9781644902837-20

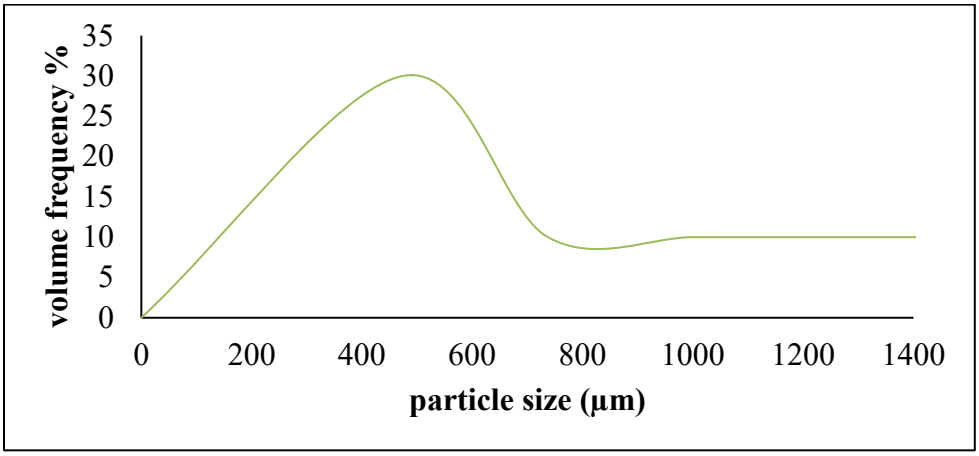

Figure 2. Particles size distribution

Results and Discussion

Figure 3 provides the outcome of DEM simulation of filling. Before the vibration starts (Fig. 3(a)) particles are segregated and separated. Larger particles mostly congregate at the inner sides due to gravity. As the vibration is begun, the particles with variety of sizes move and mix well together especially at the top region of the capsule. By longer duration of vibration, smaller particles migrate to the bottom of the capsule and improve the relative density (Fig. 3(b)) near the bottom of the capsule.

The initial RD (filled volume fraction) transferred from DEM to FEA is provided in Fig. 4 shown in discretized volumes. Figure 5 (a) shows the initial RD along with the density plot during the simulated HIP cycle compaction process. The result shows that maximum initial density is 0.6796 and the minimum density is 0.6016. Figure 5 (b) suggests that as the compact RD approaches 1, the part reaches the full densification level. As shown, the regions with more complex edges and corners demonstrate a lower RD. This suggests that the complexity of the capsule geometry and shape of the capsule affect the RD. The sharp corners and small dimension sections in both experiments and modeling may show slight deviation from full densification, due to constrained deformation/shrinkage in those areas. In parallel, a HIP capsule of the same pre-HIP capsule geometry was fabricated from mild carbon steel, filled with 316L powder, and captured pre- and post-HIP dimensions geometries via 3D laser scanning shows in Fig. 6. Comparison between FEA simulated post-HIP and experimental post-HIP dimensions are presented in Fig. 7, show acceptable result between simulation and experiment.

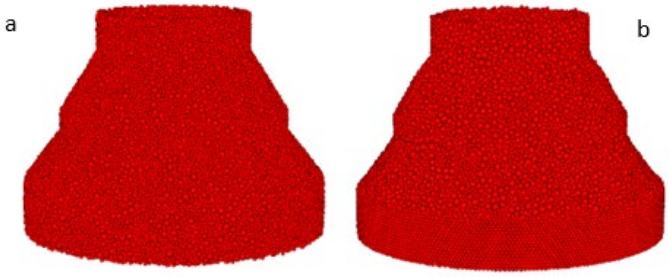

Figure 3. DEM pre-consolidation process

Materials Research Proceedings 38 (2023) 141-149 https://doi.org/10.21741/9781644902837-20

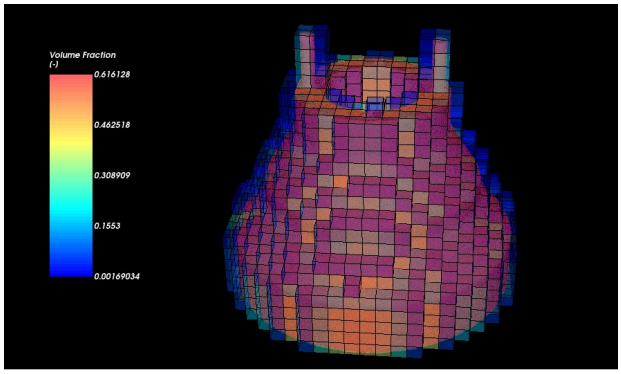

Figure 4. Volume fraction defined by Eulerian statistics exported from DEM as input to FEA

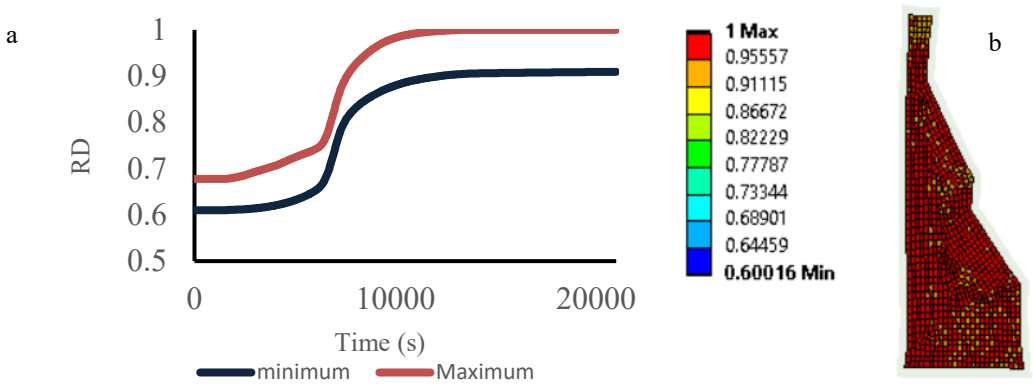

Figure 5. (a) RD plot during the HIP compaction cycle (b) final RD

Figure 6. Experimental capsule post-HIP (dots for 3D scanning)

Geometry	A	B	C	D	E	F
Post-HIP (FEM) (mm)	289.52	37.3	53.95	24.65	76.5	152.4
Post-HIP experiment (mm)	289.14	36.45	49.78	22.13	74.81	140.64
Deviation %	0.13	2.33	8.38	11.38	2.25	8.36

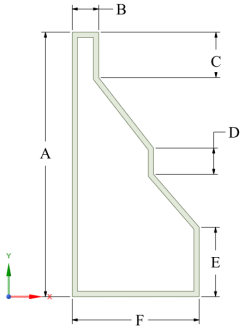

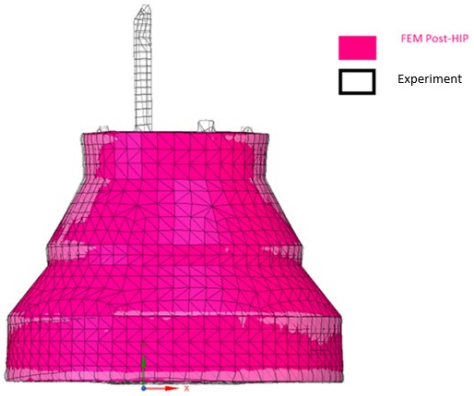

Figure 7. FEA modeling and HIP Experiment compared

Conclusions

In this study, the HIP process was modeled from the pre-consolidation stage to the final densified status. DEM was used to model the pre-consolidation filling process to establish the initial relative density (RD) of the compact, with the effects of vibration included. Finite element analysis (FEA) modeling of HIP, which includes a combined constitutive model based on compressive and consolidative mechanical behavior of powder uses the DEM results as input. The simulation predicted consolidation with an acceptable accuracy with the experiment. The result shows that full consolidation occurs with negligible deviations on sharp edges. Two additional example geometries are planned for fabrication and consolidation for further benchmarking of the simulation tool to real-world HIP component fabrication.

References

[1] Deng Y, Herzog S, Kaletsch A, Broeckmann C, Marmottant A, Laurent V. Numerical study of near-net-shape forming under encapsulation technologies and hip cladding. Proceedings Euro PM 2017: International Powder Metallurgy Congress and Exhibition 2017.

[2] Xue Y, Lang LH, Bu GL, Li L. Densification modeling of titanium alloy powder during hot isostatic pressing. Science of Sintering 2011;43:247–60. https://doi.org/10.2298/SOS1103247X

[3] Kim HS. Densification mechanisms during hot isostatic pressing of stainless steel powder compacts. Journal of Materials Processing Technology 2002;123:319–22. https://doi.org/10.1016/S0924-0136(02)00104-8

[4] Jeon YC, Kim KT. Near-net-shape forming of 316L stainless steel powder under hot isostatic pressing. International Journal of Mechanical Sciences 1999;41:815–30. https://doi.org/10.1016/S0020-7403(98)00053-8

[5] Abouaf M, Chenot JL, Raisson G, Bauduin P. Finite element simulation of hot isostatic pressing of metal powders. International Journal for Numerical Methods in Engineering 1988;25:191–212. https://doi.org/10.1002/nme.1620250116

[6] Redouani L, Boudrahem S. Hot isostatic pressing process simulation: Application to metal powders. Canadian Journal of Physics 2012;90:573–83. https://doi.org/10.1139/p2012-057

[7] Abena A, Aristizabal M, Essa K. Comprehensive numerical modelling of the hot isostatic pressing of Ti-6Al-4V powder: From filling to consolidation. Advanced Powder Technology 2019;30:2451–63. https://doi.org/10.1016/j.apt.2019.07.011

[8] Nguyen CV, Bezold A, Broeckmann C. Density distribution of powder in a HIP capsule after filling Density Distribution of Powder in a HIP Capsule after Filling 2011.

[9] Martin CL, Bouvard D. Study of the cold compaction of composite powders by the discrete element method. Acta Materialia 2003;51:373–86. https://doi.org/10.1016/S1359-6454(02)00402-0

[10] Deng Y, Kaletsch A, Bezold A, Broeckmann C. Precise Prediction of Near-Net-Shape HIP Components through DEM and FEM Modelling, 2019. https://doi.org/10.21741/9781644900031-24

[11] Zhu HP, Zhou ZY, Yang RY, Yu AB. Discrete particle simulation of particulate systems : Theoretical developments 2007;62:3378–96. https://doi.org/10.1016/j.ces.2006.12.089

[12] Elrakayby H, Kim HK, Hong SS, Kim KT. An investigation of densification behavior of nickel alloy powder during hot isostatic pressing. Advanced Powder Technology 2015;26:1314–8. https://doi.org/10.1016/j.apt.2015.07.005

[13] Harthong B, Jérier J-F, Dorémus P, Imbault D, Donzé F-V. Modeling of high-density compaction of granular materials by the Discrete Element Method. International Journal of Solids and Structures 2009;46:3357–64. https://doi.org/10.1016/j.ijsolstr.2009.05.008

[14] Van Nguyen C, Bezold A, Broeckmann C. Influence of initial powder distribution after pre-densification on the consolidation of stainless steel 316L during HIP. International Powder Metallurgy Congress and Exhibition, Euro PM 2013 2013.

[15] Van Nguyen C, Bezold A, Broeckmann C. Anisotropic shrinkage during hip of encapsulated powder. Journal of Materials Processing Technology 2015;226:134–45. https://doi.org/10.1016/j.jmatprotec.2015.06.037

[16] Khoei AR, Molaeinia Z, Keshavarz Sh. Modeling of hot isostatic pressing of metal powder with temperature–dependent cap plasticity model. Int J Mater Form 2013;6:363–76. https://doi.org/10.1007/s12289-012-1091-x

[17] Chung SH, Park H, Jeon KD, Kim KT, Hwang SM. An optimal container design for metal powder under hot isostatic pressing. Journal of Engineering Materials and Technology, Transactions of the ASME 2001;123:234–9. https://doi.org/10.1115/1.1354992

[18] Oyane M, Shima S, Kono Y. Thoery of Plasticity for Porous Metals. Bulletin of JSME 1973;16:1254–62. https://doi.org/10.1299/jsme1958.16.1254

[19] Kuhn HA, Downey CL. Material Behavior in Powder Preform Forging. ASME Pap 1972.

[20] Wikman B. Modelling and Simulation of Powder Pressing with Consideration of Friction Modelling and Simulation of Powder Pressing with Consideration of Friction 1999.

[21] Nakano M, Abe T, Kano J, Kunitomo K. DEM Analysis on Size Segregation in Feed Bed of Sintering Machine 2012;52:1559–64.

[22] Alian M, Ein-mozaffari F, Upreti SR. Analysis of the mixing of solid particles in a plowshare mixer via discrete element method (DEM). Powder Technology 2015;274:77–87. https://doi.org/10.1016/j.powtec.2015.01.012

[23] Cundall_Strack.pdf. n.d.

[24] Zhou YC, Wright BD, Yang RY, Xu BH, Yu AB. Rolling friction in the dynamic simulation of sandpile formation 1999;269:536–53.

[25] Qiao J, Duan C, Dong K, Wang W, Jiang H, Zhu H, et al. DEM study of segregation degree and velocity of binary granular mixtures subject to vibration. Powder Technology 2021;382:107–17. https://doi.org/10.1016/j.powtec.2020.12.064

[26] Walton OR, Braun RL, Walton OR, Braun RL. inelastic , frictional disks Viscosity , Granular-Temperature , and Stress Calculations for Shearing Assemblies of Inelastic , Frictional Disks * 2013;949. https://doi.org/10.1122/1.549893

[27] Chaudhuri B, Mehrotra A, Muzzio FJ, Tomassone MS. Cohesive effects in powder mixing in a tumbling blender 2006;165:105–14. https://doi.org/10.1016/j.powtec.2006.04.001

[28] Stevens AB, Hrenya CM. Comparison of soft-sphere models to measurements of collision properties during normal impacts 2005;154:99–109. https://doi.org/10.1016/j.powtec.2005.04.033

[29] Van Nguyen C, Deng Y, Bezold A, Broeckmann C. A combined model to simulate the powder densification and shape changes during hot isostatic pressing. Computer Methods in Applied Mechanics and Engineering 2017;315:302–15. https://doi.org/10.1016/j.cma.2016.10.033

[30] Deng Y, Birke C, Rajaei A, Kaletsch A, Broeckmann C. Numerical Study of Hot Isostatic Pressing with Integrated Heat Treatment of PM-HIP Cold Work Steel D7. WorldPM 2018 2018:442–53.

[31] Aryanpour G, Mashl S, Warke V. Elastoplastic-viscoplastic modelling of metal powder compaction: Application to hot isostatic pressing. Powder Metallurgy 2013;56:14–23. https://doi.org/10.1179/1743290112Y.0000000027

[32] Abouaf M, Chenot JL, Raisson G, Bauduin P. Finite element simulation of hot isostatic pressing of metal powders. International Journal for Numerical Methods in Engineering 1988;25:191–212. https://doi.org/10.1002/nme.1620250116

[33] Kuhn HA, Downey CL. Material Behavior in Powder Preform Forging. ASME Pap 1972.

[34] Kohar CP, Martin É, Connolly DS, Patil S, Krutz N, Wei D, et al. A new and efficient thermo-elasto-viscoplastic numerical implementation for implicit finite element simulations of powder metals: An application to hot isostatic pressing. International Journal of Mechanical Sciences 2019;155:222–34. https://doi.org/10.1016/j.ijmecsci.2019.01.046

[35] Group M. ANSYS USER Material Subroutine USERMAT. Technology 1999:1–22.